Письма в ЭЧАЯ. 2016. Т. 13, № 3(201). С. 497–508

TWO-LOOP ELECTROWEAK VERTEX CORRECTIONS FOR POLARIZED MØLLER SCATTERING

A. G. Aleksejevs [a,1], *S. G. Barkanova* [b,2], *Yu. M. Bystritskiy* [c,3], *E. A. Kuraev* [c], *V. A. Zykunov* [d,4]

[a] Memorial University, Corner Brook, Canada

[b] Acadia University, Wolfville, Canada

[c] Joint Institute for Nuclear Research, Dubna

[d] Belarussian State University of Transport, Gomel, Belarus

The contributions to the electron–photon vertex of two-loop electroweak corrections are calculated. The relative correction to the parity-violating asymmetry of the Møller scattering for the case of 11-GeV electron scattered off the electron at rest is found to be about –0.0034 and should be taken into account at future experiment MOLLER at JLab.

Вычислены вклады в электрон-фотонную вершину в рамках электрослабой теории в двухпетлевом приближении. Также вычислена относительная поправка к нарушающей четность асимметрии в рассеянии Мёллера. В случае рассеяния электронов с энергией 11 ГэВ на электронах мишени найден вклад в асимметрию на уровне –0,0034, что свидетельствует о том, что этот вклад должен учитываться в планируемом эксперименте MOLLER в JLab.

PACS: 12.15.Lk; 12.20.Ds; 13.40.Em

INTRODUCTION

The need for physics beyond the Standard Model (SM) is clear at least from two experimental facts: nonzero neutrino mass and the presence of dark matter in the Universe. The search for this new physics is one of the most active fields of modern physics and has three major directions: energy, cosmic and precision frontiers. The precision frontier we are interested in is driven by the indirect searches, looking for impact of new particles on observables such as scattering cross-section asymmetry causing small deviations from original SM predictions. The high-precision electroweak experiments involving the parity-violating (PV) Møller scattering, electron–positron collisions or electron–nucleon scattering can provide indirect access to new physics at multi-TeV scales and play an important complementary role in the LHC research program. These low-energy experiments tend to be less expensive than

[1]E-mail: aaleksejevs@grenfell.mun.ca
[2]E-mail: svetlana.barkanova@acadiau.ca
[3]E-mail: bystr@theor.jinr.ru
[4]E-mail: vladimir.zykunov@cern.ch

experiments at the high-energy colliders, but they do require a significant theoretical input, part of which we aim to provide in this paper.

One of such experiments, MOLLER [1], studying the parity-violating Møller scattering, would allow a determination of the weak mixing angle with an uncertainty of 0.1%, an improvement of a factor of five in fractional precision compared with the previous E158 measurement. At such precision, any inconsistency with the SM could signal new physics.

In order to match the proposed electroweak experimental precision, it is necessary to evaluate electroweak radiative corrections (EWC) on the SM observables with at least $\sim 0.1\%$ precision, which would require contributions to the electroweak cross sections of order up to $\mathcal{O}\left(\alpha^4\right)$. In the Feynman diagram approach, this corresponds to the two-loop calculations. For the MOLLER experiment, the one-loop EWC can reach up to 65% [2–5], so, although the two-loop corrections are strongly suppressed relative to the one-loop EWC, they still can potentially contribute up to a few percent. The two-loop corrections for two-to-two processes are extremely difficult to evaluate, in part because of dramatic complications due to the presence of massive vector bosons in the two-loop integrals, but they can no longer be dismissed in the new-generation precision experiments.

Starting in 2011, our group has been making a steady progress calculating major gauge-invariant two-loop contributions to the Møller parity-violating asymmetry [6–9]. We divide the two-loop EWC to the Born cross section ($\sim \mathcal{M}_0\mathcal{M}_0^+$) onto two classes: Q-part induced by quadratic one-loop amplitudes $\sim \mathcal{M}_1\mathcal{M}_1^+$, and T-part — the interference of Born and two-loop amplitudes $\sim 2\,\mathrm{Re}\,\left(\mathcal{M}_0\mathcal{M}_2^+\right)$ (here index i in the amplitude $\mathcal{M}_i$ corresponds to the order of perturbation theory). The Q-part was calculated exactly in [6] (using the Feynman–'t Hooft gauge and the on-shell renormalization), where we show that the Q-part is much higher than the planned experimental uncertainty of MOLLER; i.e., the two-loop EWC are larger than was assumed in the past. The large size of the Q-part demands detailed and consistent treatment of the T-part, but this formidable task will require several stages. Our first step was to calculate the gauge-invariant double boxes [7]. In paper [9], we considered the EWC arising from the contribution of a wide class of the gauge-invariant Feynman amplitudes of the box type with one-loop insertions: fermion mass operators (or Fermion Self-Energies in Boxes), vertex functions (or Vertices in Boxes), and polarization of vacuum for bosons (or Boson Self-Energies in Boxes). In this paper, we do the next step — we calculate the insertions of two-loop vertices to vertices (VV), fermion self-energies to vertices (FSEV), and double vertices (DV).

The paper is organized as follows. In Sec. 1, we consider the asymmetry in the Born approximation and introduce the basic notations. In Sec. 2, we calculate two Feynman diagrams with extra W- and Z-boson subgraphs (VV). Section 3 is devoted to the diagrams with lepton mass operators insertions (FSEV). We consider complex vertices (DV) in Sec. 4 and give numerical estimation of total effect of these contributions in Sec. 5.

1. BASIC NOTATIONS

We consider the process of electron–electron elastic scattering, i.e., the Møller process:

$$e(p_1, \lambda_1) + e(p_2, \lambda_2) \to e(p_1', \lambda_1') + e(p_2', \lambda_2'), \tag{1}$$

where $\lambda_{1,2}$ ($\lambda_{1,2}'$) are the chiral states of initial (final) electrons and $p_{1,2}$ are 4-momenta of initial electrons and $p_{1,2}'$ are 4-momenta of final electrons. The first measurement of the parity-violating (left–right) asymmetry

$$A = \frac{d\sigma^{----} - d\sigma^{++++}}{d\sigma^{----} + d\sigma^{++++} + d\sigma^{+-+-} + d\sigma^{+--+} + d\sigma^{-+-+} + d\sigma^{-++-}} = \\ = \frac{|M^{----}|^2 - |M^{++++}|^2}{\sum\limits_{\lambda} |M^{\lambda}|^2} \quad (2)$$

in the Møller scattering was made by E158 experiment at SLAC [10–12]. In the lowest order of perturbation theory in the framework of QED, the matrix element squared which is summed over polarization states of electrons has the following form:

$$\sum_{\lambda} |M^{\lambda}|^2 = 8(4\pi\alpha)^2 \frac{s^4 + t^4 + u^4}{t^2 u^2}. \quad (3)$$

We use the notation for the kinematic invariants neglecting the electron mass m:

$$s = 2p_1 p_2, \quad t = -2p_1 p_1', \quad u = -2p_1 p_2', \quad s + t + u = 0. \quad (4)$$

Thus, here and further we neglect the terms of order $O(m^2/s)$ since in MOLLER experiment it is expected that beam energy is $E_{\text{beam}} = 11$ GeV, that is $s = 2mE_{\text{beam}} \approx 0.01124$ GeV^2. Sometimes we retain electron mass at intermediate steps of calculations, but in final results it survives only as the arguments of collinear logarithm (in form $\ln\left(s/m^2\right)$). Within the Standard Model one has additional contribution in the Born approximation with Z-boson exchange which gives rise to polarization asymmetry A^0:

$$A^0 = \frac{s}{2m_W^2} A_{(0)} \frac{a}{s_W}, \qquad A_{(0)} = \frac{y(1-y)}{1 + y^4 + (1-y)^4}, \qquad y = \frac{-t}{s} = \frac{1-c}{2}, \quad (5)$$

where $c = \cos\theta$ is the cosine of scattering angle $\theta = \left(\widehat{\mathbf{p}_1, \mathbf{p}_1'}\right)$ in the system of center-of-mass of electrons; m_W is the W-boson mass, and a is the so-called "weak electron charge"

$$a = 1 - 4s_W^2. \quad (6)$$

Now let us recall that s_W (c_W) is the sine (cosine) of the Weinberg angle expressed in terms of the Z- and W-boson masses according to the Standard Model rules:

$$s_W = \sqrt{1 - c_W^2}, \qquad c_W = \frac{m_W}{m_Z}. \quad (7)$$

Thus, the factor a is just $a \approx 0.109$, and the asymmetry is, therefore, suppressed by both s/m_W^2 and a. Even at Central Region (CR) of MOLLER (at $\theta \sim 90^\circ$, i.e., $t \approx u \approx -s/2$), where the Born asymmetry is maximal, this asymmetry is extremely small

$$A^0 = \frac{s}{9m_W^2} \frac{a}{s_W^2} \approx 9.4968 \cdot 10^{-8}. \quad (8)$$

It is the main aim of this paper to estimate the contribution of some classes of two-loop contributions, which have some logarithmical enhancement. As for the non-enhanced ones —

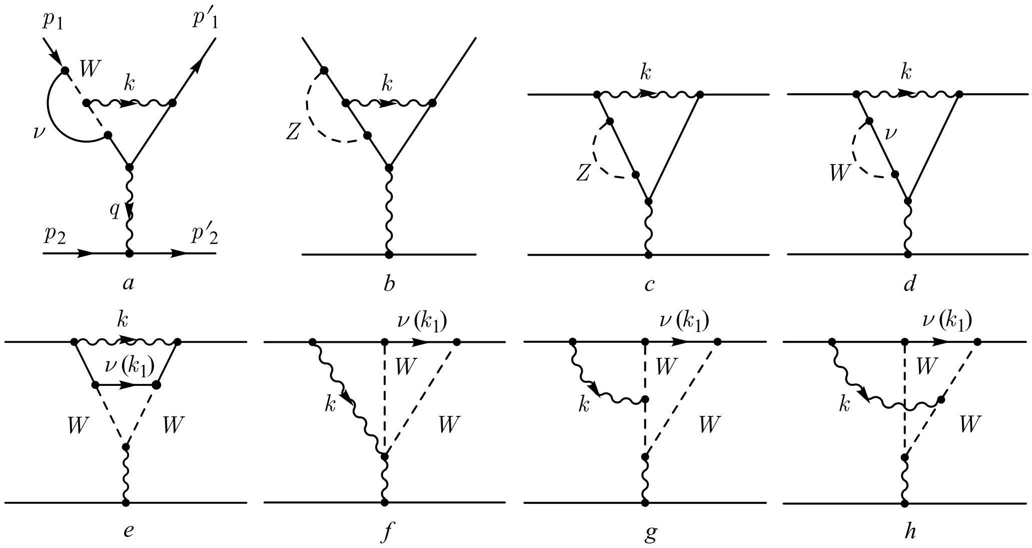

Two-loop vertices to vertices (a, b), fermion self-energies to vertices (c, d), double vertices (e–h). Photons are denoted by wavy lines, massive bosons — by dashed lines, electrons and neutrinos — by solid lines. Notations on diagrams show the type of particle (Z, W, ν) and 4-momenta of them

they have an order of $(-t/m_Z^2)(\alpha/\pi)^2 \approx 10^{-11}$ for CR of MOLLER. Below we consider contribution to the vertex function ΔV_μ for on-mass-shell electrons $p_1^2 = p_1'^2 = m^2$ and the space-like 4-momentum of the virtual photon $Q^2 = -q^2 = -(p_1 - p_1')^2 \gg m^2$ in two-loop level from the class of the Feynman diagrams containing the intermediate states with W and Z bosons (see the Figure). Due to vertex renormalization condition $\Delta V_\mu|_{Q^2=0} = 0$, the corresponding contribution is proportional to $Q^2/m_{W,Z}^2$. Thus, we restrict ourselves by the condition

$$\rho_i^{-1} = \frac{Q^2}{m_i^2} \ll 1, \qquad i = W, Z. \tag{9}$$

2. VERTEX SUBGRAPHS WITH EXTRA W AND Z BOSONS

The one-loop expression for contribution of $WW\gamma$ vertex to $e(p_1) \to e(p_1 - k) + \gamma(k)$ vertex (see Fig. a) has the form

$$V_\mu^a(p_1, k) = -ie\bar{u}(p_1 - k)\gamma_\mu\omega_- u(p_1)\frac{g^2}{32\pi^2} I^a(k^2), \tag{10}$$

$$I^a(k^2) = \int_0^1 dy \int_0^y dx \left(6 \ln \frac{m_W^2 y - k^2 x\bar{x}}{m_W^2 y} + \frac{k^2 x(1-2x)}{m_W^2 y - k^2 x\bar{x}}\right), \tag{11}$$

where $\omega_\pm = 1 \pm \gamma_5$, $g = e/s_W$, and e is the electron charge value ($e = |e| > 0$). Here and below we use the common notation $\bar{x} \equiv 1 - x$, $\bar{y} \equiv 1 - y$, etc. Analogously, one-loop vertex with one additional Z boson (see corresponding subgraph in Fig. b) looks like

$$V_\mu^b(p_1,k) = -ie\bar{u}(p_1-k)\gamma_\mu(a\pm\gamma_5)^2u(p_1)\frac{g^2}{(4c_W)^2 16\pi^2}I^b(k^2), \tag{12}$$

$$I^b(k^2) = \int\limits_0^1 dy \int\limits_0^y dx\left(-2\ln\frac{m_Z^2\bar{y}-k^2x\bar{x}}{m_Z^2\bar{y}} + \frac{k^2x\bar{x}}{m_Z^2\bar{y}-k^2x\bar{x}}\right). \tag{13}$$

Both functions $I^{a,b}(k^2)$ are normalized as $I^{a,b}(0)=0$.

Integrating over 4-momenta of photon k, we get the contribution of (10) into full two-loop vertex V_μ (see Fig. a) as

$$\begin{aligned} \Delta V_\mu^a &= -ie\frac{g^2 4\pi\alpha}{(16\pi^2)^2}I_\mu^a, \\ I_\mu^a &= I_{1\mu}^a + I_{2\mu}^a = \int\frac{d^4k}{i\pi^2}\frac{N_\mu^a}{k^2(k^2-2p_1k)(k^2-2p_1'k)}I^a(k^2), \end{aligned} \tag{14}$$

$$N_\mu^a = \bar{u}(p_1')\gamma_\lambda(\hat{p}_1'-\hat{k}+m)\gamma_\mu(\hat{p}_1-\hat{k}+m)\gamma^\lambda\omega_- u(p_1), \tag{15}$$

where two terms $I_{1,2\mu}^a$ in (14) correspond to two terms in (11). Omitting the terms of order $\mathcal{O}(\rho_i^{-2})$, we write down the contribution $I_{1\mu}^a$ as

$$I_{1\mu}^a = 6\int\limits_0^1 y\bar{y}\,dy\int\frac{d^4k}{i\pi^2}\left.\frac{N_\mu^a}{m_W^2(k^2-2p_1k)(k^2-2p_1'k)}\right|_{|k^2|\ll m_W^2}. \tag{16}$$

Using the Feynman parameters trick, one can integrate over loop momenta k and obtain the result as a sum of ultraviolet finite (UV-finite) and ultraviolet divergent (UVD) parts:

$$\frac{Q^2}{m_W^2}\int\limits_0^1 x\bar{x}\left(\ln\frac{m_W^2}{b^2}-1\right)dx + \text{UVD-part},$$

where $b^2 = (p_1x+p_1'\bar{x})^2 = m^2+Q^2x\bar{x}$. Here and below we use the same notations for unrenormalized and renormalized quantities. Thus, after renormalization of $I_{1\mu}^a$, we obtain the expression

$$I_{1\mu}^a = \frac{Q^2}{m_W^2}c_1^a\bar{u}(p_1')\gamma_\mu\omega_- u(p_1), \qquad c_1^a = \frac{1}{3}\ln\frac{m_W^2}{Q^2}+\frac{7}{18} = 5.0406. \tag{17}$$

Here and everywhere below the number value corresponds to CR of MOLLER.

Second term $I_{2\mu}^a$ in (14) can be written as

$$I_{2\mu}^a = \int\limits_0^1 y\bar{y}\,dy\int\limits_0^y dx\frac{1-2x}{1-x}\int\frac{d^4k}{i\pi^2}\frac{N_\mu^a}{(k^2-\sigma^2)(k^2-2p_1k)(k^2-2p_1'k)}, \tag{18}$$

where $\sigma^2 = m_W^2 y/(x\bar{x})$. Again using standard manipulations, we arrive at

$$I_{2\mu}^a = \bar{u}(p_1')\gamma_\mu\omega_- u(p_1)\int\limits_0^1 y\bar{y}\,dy\int\limits_0^y dx\frac{1-2x}{1-x}\int\limits_0^1 dx_1\int\limits_0^1 2y_1\,dy_1\times$$

$$\times\left[\ln\frac{\Lambda^2}{D_a}-\frac{3}{2}-\frac{Q^2}{D_a}(1-y_1x_1)(1-y_1\bar{x}_1)\right], \quad (19)$$

where $D_a = y_1^2 b_a^2 + \sigma^2\bar{y}_1$, $b_a^2 = (x_1p_1+\bar{x}_1p_1')^2 = m^2 + x_1\bar{x}_1Q^2$, and Λ is the UV-regularization parameter. Applying the renormalization procedure, we obtain

$$I_{2\mu}^a = \frac{Q^2}{m_W^2}c_2^a\bar{u}(p_1')\gamma_\mu\omega_- u(p_1),$$

$$c_2^a = -\int\limits_0^1 dx_1\int\limits_0^1 2y_1\,dy_1\int\limits_0^1 y\bar{y}\,dy\int\limits_0^y dx\frac{1-2x}{1-x}\times \quad (20)$$

$$\times\left[\rho_W\ln\left(1+\frac{1}{\rho_W}\frac{x_1\bar{x}_1y_1^2x\bar{x}}{y\bar{y}_1}\right)+\frac{\rho_W x\bar{x}(1-y_1x_1)(1-y_1\bar{x}_1)}{\rho_W y\bar{y}_1+y_1^2x\bar{x}x_1\bar{x}_1}\right] = -0.0930.$$

The final expression for contribution of W-vertex subgraph to the vertex function (see Fig. *a*) is

$$\Delta V_\mu^a = -ie\frac{Q^2}{m_W^2}\frac{g^2 4\pi\alpha}{(16\pi^2)^2}(c_1^a+c_2^a)\bar{u}(p_1')\gamma_\mu\omega_- u(p_1). \quad (21)$$

Contribution of Z-vertex subgraph (see Fig. *b*) has the form

$$\Delta V_\mu^b = -ie\frac{g^2 8\pi\alpha}{(4c_W)^2(16\pi^2)^2}I_\mu^b,$$

$$I_\mu^b = \int\frac{d^4k}{i\pi^2}\frac{N_\mu^b}{k^2(k^2-2p_1k)(k^2-2p_1'k)}I^b(k^2), \quad (22)$$

$$N_\mu^b = \bar{u}(p_1')\gamma_\lambda(\hat{p}_1'-\hat{k}+m)\gamma_\mu(\hat{p}_1-\hat{k}+m)\gamma_\lambda(a\pm\gamma_5)^2u(p_1).$$

In the similar way, we obtain for contribution of Z-vertex subgraph to the vertex function

$$\Delta V_\mu^b = -ie\frac{Q^2}{m_Z^2}\frac{g^2 8\pi\alpha(1\pm a)^2}{(4c_W)^2(16\pi^2)^2}(c_1^b+c_2^b)\bar{u}(p_1')\gamma_\mu u(p_1), \quad (23)$$

where

$$c_1^b = \frac{2}{9}\ln\frac{m_Z^2}{Q^2}+\frac{7}{27} = 3.4164,$$

$$c_2^b = -\int\limits_0^1 dx_1\int\limits_0^1 2y_1\,dy_1\int\limits_0^1 y\bar{y}\,dy\int\limits_0^y dx\frac{1-2x}{1-x}\times$$

$$\times\left[\rho_Z\ln\left(1+\frac{1}{\rho_Z}\frac{x_1\bar{x}_1y_1^2x\bar{x}}{y\bar{y}_1}\right)+\frac{\rho_Z x\bar{x}(1-y_1x_1)(1-y_1\bar{x}_1)}{\rho_Z y\bar{y}_1+y_1^2x\bar{x}x_1\bar{x}_1}\right] = -0.0944. \quad (24)$$

3. ELECTROWEAK ELECTRON MASS OPERATOR INSERTION TO THE VERTEX FUNCTION

Now let us consider the set of the Feynman diagrams of vertex type containing electron Mass Operator (MO) with internal Z- or W-bosons insertions (see Fig. c, d). The relevant contribution to the vertex function has the form

$$\Delta V_\mu^{\rm MO} = -ie\frac{\alpha}{2\pi}\left[V_\mu^Z + V_\mu^W\right], \quad V_\mu^i = \int \frac{d^4k}{i\pi^2}\frac{N_\mu^i}{k^2(k^2-2p_1'k)}, \tag{25}$$

where $i = Z, W$, and the numerator N_μ^i is

$$N_\mu^i = \bar{u}(p_1')\gamma_\lambda(\hat{p}_1' - \hat{k} + m)\gamma_\mu(\hat{p}_1 - \hat{k} + m)\gamma^\lambda c^{(i)} u(p_1) M^i(k, p_1), \tag{26}$$

with

$$c^{(Z)} = \frac{2g^2(a \pm \gamma_5)^2}{(4c_W)^2 8\pi^2}, \quad c^{(W)} = \frac{g^2\omega_-}{16\pi^2}. \tag{27}$$

Mass operator $M^i(k, p_1)$ of the off-mass-shell electron looks like

$$M^i(k, p_1) = \int\limits_0^1 x_1\bar{x}_1\, dx_1 \int\limits_0^1 \frac{dz}{m_i^2 - x_1 z(k^2 - 2p_1k)}. \tag{28}$$

The standard Feynman procedure of joining the denominators and the loop momentum integrating gives us

$$\begin{gathered} V_\mu^i = \int\limits_0^1 \bar{x}_1\, dx_1 \int\limits_0^1 \frac{dz}{z} \int \frac{d^4k}{i\pi^2}\frac{N_\mu}{k^2(k^2-2p_1'k)(k^2-2p_1k-\sigma_i^2)}, \\ N_\mu = \bar{u}(p_1')\gamma_\lambda(\hat{p}_1' - \hat{k} + m)\gamma_\mu(\hat{p}_1 - \hat{k} + m)\gamma_\lambda u(p_1), \quad \sigma_i^2 = \frac{m_i^2}{x_1 z}, \end{gathered} \tag{29}$$

which can be simplified to the form

$$\begin{gathered} V_\mu^i = \bar{u}(p_1')\gamma_\mu u(p_1) V_i, \\ V_i = \int\limits_0^1 \bar{x}_1\, dx_1 \int\limits_0^1 \frac{dz}{z} \int\limits_0^1 dx \int\limits_0^1 2y\, dy \left(\ln\frac{\Lambda^2}{D_i} - \frac{Q^2}{D_i}\right), \end{gathered} \tag{30}$$

where $D_i = b^2y^2 + xy\sigma_i^2$. After renormalization and expansion on powers of Q^2/m_i^2, we obtain

$$V_i = -\frac{Q^2}{m_i^2}\int\limits_0^1 \bar{x}_1\, dx_1 \int\limits_0^1 \frac{dz}{z}\int\limits_0^1 dx \int\limits_0^1 2y\, dy \left[x_1 zy\bar{x} + \frac{m_i^2}{D_i}(\bar{y} - y^2 x\bar{x})\right]. \tag{31}$$

Final expression for the contribution to the vertex function (see Fig. *c*, *d*) is

$$\Delta V_\mu^{\mathrm{MO}} = ie\frac{\alpha}{2\pi}\left[\frac{Q^2}{m_Z^2}c_3^Z\frac{g^2}{(4c_W)^2 4\pi^2}(1\pm a)^2\bar{u}(p_1')\gamma_\mu u(p_1) + \right.$$
$$\left. + \frac{Q^2}{m_W^2}c_3^W\frac{g^2}{16\pi^2}\bar{u}(p_1')\gamma_\mu\omega_- u(p_1)\right], \quad (32)$$

with

$$c_3^Z = \frac{1}{6}\ln\frac{m_Z^2}{Q^2} + \frac{2}{3} = 3.0345, \quad c_3^W = \frac{1}{6}\ln\frac{m_W^2}{Q^2} + \frac{2}{3} = 2.9925. \quad (33)$$

4. CONTRIBUTION OF DIAGRAMS CONTAINING $WW\gamma$, $WW\gamma\gamma$ VERTICES

Below we consider diagrams containing $WW\gamma\gamma$, $WW\gamma$ vertices only because their contributions are associated with logarithmic enhancement. Let us consider the Feynman diagram with virtual photon which is emitted from the initial electron and absorbed by the final electron (see Fig. *e*). The relevant contribution to the vertex function is

$$\Delta V_\mu^e = ie\frac{4\pi\alpha g^2}{2(16\pi^2)^2}V_\mu^e,$$
$$V_\mu^e = \int\frac{d^4k}{i\pi^2}\frac{1}{(k^2-\lambda^2)(k^2-2p_1k)(k^2-2p_1'k)}\times \quad (34)$$
$$\times\int\frac{d^4k_1}{i\pi^2}\frac{V_{\sigma\mu\eta}N^{\eta\sigma}}{k_1^2((k+k_1-p_1)^2-m_W^2)((k+k_1-p_1')^2-m_W^2)},$$

where λ is the photon mass, and

$$V_{\sigma\mu\eta} = g_{\sigma\mu}(2p_1-p_1'-k-k_1)_\eta + g_{\mu\sigma}(2p_1'-p_1-k-k_1)_\sigma +$$
$$+ g_{\eta\sigma}(-p_1-p_1'+2(k+k_1))_\mu, \quad (35)$$
$$N_{\eta\sigma} = \bar{u}(p_1')\gamma_\lambda(\hat{p}_1'-\hat{k})\gamma_\eta\hat{k}_1\gamma_\sigma(\hat{p}_1-\hat{k})\gamma^\lambda\omega_- u(p_1).$$

Doing the similar treatment as it was done above, one can integrate over loop momentum k_1, renormalize the amplitude of this subgraph and obtain

$$V_\mu^e = \frac{3Q^2}{2m_W^2}\int\frac{d^4k}{i\pi^2}\left.\frac{\bar{u}(p_1')\gamma_\lambda(\hat{p}_1'-\hat{k})\gamma_\mu(\hat{p}_1-\hat{k})\gamma^\lambda\omega_- u(p_1)}{(k^2-\lambda^2)(k^2-2p_1k)(k^2-2p_1'k)}\right|_{|k^2|\ll m_W^2}. \quad (36)$$

After integration over k one gets

$$V_\mu^e = \frac{3Q^2}{2m_W^2}\int_0^1 dx\int_0^1 2y\,dy\left[\ln\frac{m_W^2}{D_e} - \frac{Q^2}{D_e}(\bar{y}+y^2x\bar{x})\right], \quad (37)$$

where $D_e = y^2 b^2 + \lambda^2 \bar{y}$. Further, we use simple integrals

$$\int_0^1 \frac{2y\,dy}{y^2 b^2 + \lambda^2 \bar{y}} = \frac{1}{b^2} \ln \frac{b^2}{\lambda^2}, \qquad \int_0^1 \frac{Q^2}{b^2} dx = 2 \ln \frac{Q^2}{m^2},$$

$$\int_0^1 \frac{Q^2 x \bar{x}}{b^2} dx = 1, \qquad \int_0^1 \frac{Q^2}{b^2} \ln \frac{b^2}{m^2}\, dx = \ln^2 \frac{Q^2}{m^2} - \frac{\pi^2}{3}$$

and obtain

$$\Delta V_\mu^e = ie \frac{3Q^2}{2m_W^2} \bar{u}(p_1') \gamma_\mu \omega_- u(p_1) \frac{4\pi\alpha g^2}{2(16\pi^2)^2} I^e,$$

$$I^e = 2 + \frac{\pi^2}{3} + \ln \frac{m_W^2}{Q^2} - 2 \ln \frac{Q^2}{m^2} \left(\ln \frac{m^2}{\lambda^2} - 2 \right) - \ln^2 \frac{Q^2}{m^2} = -2 \ln \frac{Q^2}{m^2} \ln \frac{m^2}{\lambda^2} - 40.388. \tag{38}$$

The diagrams in Figs.*f–h* have a general enhancement factor which is associated with the collinear photon emission in vertex. Let us demonstrate this in general. The common structure for all three diagrams contains the emission of photon with momentum k from initial electron. This leads to the following structure of the amplitude:

$$V_\mu^{f,g,h} = \frac{e}{16\pi^2} \int \frac{d^4 k}{i\pi^2} \frac{\bar{u}(p_1') O_\mu^\lambda (\hat{p}_1 - \hat{k} + m) \gamma_\lambda u(p_1)}{k^2 (k^2 - 2p_1 k)}, \tag{39}$$

where O_μ^λ corresponds to the remaining part of the Feynman diagram and is different for each diagram. We note that the dominant contribution to this integral comes from the integration region of small photon momentum (i.e., $|k^2| \ll m_W^2$), and thus we can omit k in the remaining part of vertex amplitude, containing the momenta of a W boson. Joining the denominators, we have

$$V_\mu^{f,g,h} = \frac{e}{16\pi^2} \int_0^1 dx\, 2\bar{x}\, \bar{u}(p_1') p_{1\lambda}\, O_\mu^\lambda \big|_{k \sim x p_1} u(p_1) \int \frac{d^4 k}{i\pi^2} \left. \frac{1}{((k - x p_1)^2 - m^2 x^2)^2} \right|_{|k^2| \ll m_W^2},$$

where we approximated the traces of the amplitude by taking it in collinear region (i.e., putting $k \to x p_1$). This gives us the possibility to integrate over $d^4 k$ and obtain

$$V_\mu^{f,g,h} \approx \frac{e}{16\pi^2} \int_0^1 dx\, 2\bar{x}\, \bar{u}(p_1') p_{1\lambda}\, O_\mu^\lambda \big|_{k \sim x p_1} u(p_1) \left(\ln \frac{m_W^2}{m^2 x^2} - 1 \right). \tag{40}$$

The diagram containing the $WW\gamma\gamma$ vertex (see Fig.*f*) gives

$$\Delta V_\mu^f = 2ieR \frac{4\pi\alpha g^2}{32\pi^2} S_{\mu\nu}{}^{\lambda\sigma} p_1^\nu \int \frac{d^4 k_1}{i\pi^2} \frac{N_{\lambda\sigma}^f}{k_1^2 (k_1^2 - 2p_1 k_1 - m_W^2)(k_1^2 - 2p_1' k_1 - m_W^2)}, \tag{41}$$

$$N_{\lambda\sigma}^f = \bar{u}(p_1') \gamma_\sigma \hat{k}_1 \gamma_\lambda \omega_- u(p_1), \quad S_{\mu\nu\lambda\sigma} = 2g_{\mu\nu} g_{\lambda\sigma} - g_{\mu\lambda} g_{\nu\sigma} - g_{\mu\sigma} g_{\nu\lambda},$$

$$R \approx \frac{e}{16\pi^2} L, \quad L = \ln \frac{m_W^2}{m^2}.$$

The loop momentum integral does not have ultraviolet as well as infrared divergences. Standard manipulations lead to

$$\Delta V_\mu^f = 2ie\frac{Q^2}{4m_W^2}\frac{4\pi\alpha g^2}{2(16\pi^2)^2}\,L\,\bar{u}(p_1')\gamma_\mu\omega_- u(p_1). \tag{42}$$

For the Feynman diagram with $WW\gamma$ vertex shown in Fig. g we have

$$\Delta V_\mu^g = -2iR\frac{4\pi\alpha g^2}{32\pi^2}\int\frac{d^4k_1}{i\pi^2}\frac{\bar{u}(p_1')\gamma_\eta\hat{k}_1\gamma_\lambda\omega_- u(p_1)V_1^{\lambda\nu\sigma}{V_2}_\mu^{\ \eta\sigma}\ p_{1\nu}}{k_1^2\left(k_1^2-2p_1k_1-m_W^2\right)^2\left(k_1^2-2p_1'k_1-m_W^2\right)}, \tag{43}$$

where vertices have the form

$$\begin{aligned} V_1^{\lambda\nu\sigma} &= (2p_1-k_1)^\lambda g^{\nu\sigma}+(2k_1-p_1)^\nu g^{\sigma\lambda}+(-p_1-k_1)^\sigma g^{\lambda\nu},\\ {V_2}_\mu^{\ \eta\sigma} &= (-p_1-p_1'+2k_1)_\mu g^{\eta\sigma}+(2p_1-p_1'-k_1)^\eta g_\mu^\sigma+(2p_1'-p_1-k_1)^\sigma g_\mu^\eta. \end{aligned} \tag{44}$$

Retaining in the numerator the terms quadratic over loop momenta, one gets

$$\Delta V_\mu^g = -iR\frac{\alpha g^2}{2\pi}\bar{u}(p_1')\,\gamma_\mu\omega_- u(p_1)\int\limits_0^1 x\,dx\int\limits_0^1 y^2\,dy\frac{Q^2}{D_g}\left(-\frac{13}{4}\right), \tag{45}$$

where $D_g \approx ym_W^2$. Finally, we have for the contribution of the Feynman diagram shown in Fig. g:

$$\Delta V_\mu^g = -ie\frac{Q^2}{m_W^2}\,L\,\frac{\alpha g^2}{32\pi^3}\frac{13}{36}\,\bar{u}(p_1')\,\gamma_\mu\omega_- u(p_1), \tag{46}$$

and the diagram shown in Fig. h gives the similar result:

$$\Delta V_\mu^h = -ie\frac{Q^2}{m_W^2}\,L\,\frac{\alpha g^2}{64\pi^3}\frac{67}{36}\,\bar{u}(p_1')\,\gamma_\mu\omega_- u(p_1). \tag{47}$$

5. NUMERICAL CONTRIBUTION TO THE LEFT–RIGHT ASYMMETRY

Collecting the result of considered two-loop contributions, one can put the total result in the form

$$\Delta V_\mu^{a+b}+\Delta V_\mu^{\rm MO}+\Delta V_\mu^{e+f+g+h} = B^Z K_\mu^Z + B^W K_\mu^W, \tag{48}$$

where

$$K_\mu^Z = ie\frac{Q^2}{m_Z^2}(1\pm a)^2\frac{\alpha g^2}{(4c_W)^2 256\pi^3}\bar{u}(p_1')\gamma_\mu u(p_1), \tag{49}$$

$$K_\mu^W = ie\frac{Q^2}{m_W^2}\frac{\alpha g^2}{256\pi^3}\bar{u}(p_1')\gamma_\mu\omega_- u(p_1), \tag{50}$$

and the coefficients look like

$$B^Z = -8(c_1^b + c_2^b) + 32c_3^Z = 70.5285,$$
$$B^W = -4(c_1^a + c_2^a) + 8c_3^W + 3I^{e,\text{fin}} + L\left(1 - \frac{26}{9} - \frac{67}{9}\right) = -312.382. \tag{51}$$

Let us note by index C the contributions investigated here, i.e., $C = a, b, \ldots, h$. As specific corrections to observable parity-violating asymmetry induced by contribution C we choose the contribution to the asymmetry $(\Delta A)_C$ and the relative corrections D_A^C:

$$(\Delta A)_C = \frac{|\mathcal{M}_C^{----}|^2 - |\mathcal{M}_C^{++++}|^2}{\sum |\mathcal{M}_0^\lambda|^2}, \tag{52}$$

$$D_A^C = \frac{(\Delta A)_C}{A^0} = \frac{|\mathcal{M}_C^{----}|^2 - |\mathcal{M}_C^{++++}|^2}{|\mathcal{M}_0^{----}|^2 - |\mathcal{M}_0^{++++}|^2}. \tag{53}$$

The physical effect of radiative effects from contribution C to observable asymmetry is determined by the relative correction (see [9] for more details):

$$\delta_A^C = \frac{A^C - A^0}{A^0} = \frac{D_A^C - \delta^C}{1 + \delta^C}, \tag{54}$$

where the relative correction to unpolarized cross section is $\delta^C = \sigma_{00}^C/\sigma_{00}^0$. For two-loop effects (where δ^C is small) the approximate equation for relative correction to asymmetry takes place: $\delta_A^C \approx D_A^C$.

Contributions to asymmetry of Z and W types are

$$(\Delta A)_Z = -16aB^Z \frac{Q^2}{m_Z^2} \frac{\alpha g^2 \pi}{(4c_W)^2(16\pi^2)^2},$$
$$(\Delta A)_W = 4B^W \frac{Q^2}{m_W^2} \frac{\alpha g^2 \pi}{(16\pi^2)^2}, \tag{55}$$

which give the relevant numerical values

$$(\Delta A)_Z = -2.5410 \cdot 10^{-12}, \quad (\Delta A)_W = -3.1983 \cdot 10^{-10}. \tag{56}$$

Taking into account that in CR of MOLLER the Born asymmetry $A^0 = 94.97$ ppb, the numbers for relative corrections D_A^C are

$$D_A^Z = -0.0000267, \quad D_A^W = -0.0033677. \tag{57}$$

We can see that effects have the same negative sign, the first is rather small, but the second one is at the edge of the region of planned one per cent experimental error for MOLLER, and thus will be important for future analysis of MOLLER experimental results.

Acknowledgements. Many thanks to Prof. A. B. Arbuzov and Prof. D. Yu. Bardin for help and valuable discussions. The work of A. G. A. and S. G. B. has been supported by the Natural Science and Engineering Research Council of Canada (NSERC). Yu. M. B. acknowledges support of Heisenberg–Landau Program grant No. HLP-2015-15. V. A. Z. is grateful to the financial support of Belarus program "Convergence" (No. 20141163) and thanks JINR for hospitality in 2014, 2015.

REFERENCES

1. *Benesch J. et al. (MOLLER Collab.).* The MOLLER Experiment: An Ultra-Precise Measurement of the Weak Mixing Angle Using Møller Scattering. arXiv:1411.4088.
2. *Aleksejevs A. G. et al.* Electroweak Radiative Corrections for Polarized Møller Scattering at Future 11 GeV JLab Experiment // Phys. Rev. D. 2010. V. 82. P. 093013.
3. *Aleksejevs A. G., Barkanova S. G., Zykunov V. A.* Precise Calculations of Observables of Polarized Møller Scattering: From Jlab to ILC Energies // Phys. At. Nucl. 2012. V. 75. P. 209.
4. *Aleksejevs A. G. et al.* One-Loop Electroweak Corrections for Polarized Møller Scattering at Different Renormalization Schemes and Conditions // Phys. Part. Nucl. 2013. V. 44. P. 161.
5. *Zykunov V. A.* Radiative Møller Scattering Involving Polarized Particles // Phys. At. Nucl. 2015. V. 78. P. 453.
6. *Aleksejevs A. G. et al.* Quadratic Electroweak Corrections for Polarized Møller Scattering // Phys. Rev. D. 2012. V. 85. P. 013007.
7. *Aleksejevs A. G. et al.* Parity-Violating Møller Scattering Asymmetry up to the Two-Loop Level. arXiv:1202.0378.
8. *Aleksejevs A. G. et al.* Estimating Two-Loop Radiative Effects in the MOLLER Experiment // Phys. At. Nucl. 2013. V. 76. P. 888.
9. *Aleksejevs A. G. et al.* NNLO Electroweak Corrections for Polarized Moeller Scattering: One-Loop Insertions to Boxes // Phys. Part. Nucl. Lett. 2015. V. 12. P. 645.
10. *Kumar K. S. et al.* Precision Low-Energy Weak Neutral Current Experiments // Mod. Phys. Lett. A. 1995. V. 10. P. 2979.
11. *Kumar K.* The E158 Experiment // Eur. Phys. J. A. 2007. V. 32. P. 531.
12. *Anthony P. et al. (SLAC E158 Collab.).* Observation of Parity Nonconservation in Møller Scattering // Phys. Rev. Lett. 2004. V. 92. P. 181602.

Received on September 3, 2015.